Progress In Electromagnetics Research B, Vol. 59, 103–121, 2014

Real Time Implementation for DOA Estimation Methods on NI-PXI Platform

Nizar Tayem*

Abstract—In this paper, we present five different approaches to estimate direction of arrival (DOA) of multiple incident RF sources. The proposed methods are based on extracting the signal and noise subspaces from the Q matrix, R matrix, or both Q and R matrices of the QR decomposed received data matrix. The angle of the signal arrival is extracted from the signal subspace by using similar techniques as employed by MUSIC and ESPRIT methods. The simulation results are shown which verify accurate DOA estimates for both single and two sources. In addition, an experimental verification of the proposed methods is also presented. The methods are implemented in LabVIEW software and a prototype is built using National Instruments (NI) hardware. Furthermore, the details of experimental procedures are presented which includes interfacing the uniform linear array (ULA) of antennas with the NI-PXI platform, phase difference calibration between the RF receivers, and selection of transmitter and receiver parameters. The experimental results are shown for a single and two RF sources lying at arbitrary angles from the array reference, which verify the successful real-time implement-ability of the proposed DOA estimation methods.

1. INTRODUCTION

The problem of estimating the bearing angles of multiple incident RF sources has always attracted the interests of researchers due to its innumerable practical applications in radar and sonar for source localization, and beam forming/steering in mobile communication. The existing literature in this area focuses primarily on finding ways to improve the precision and reduce the complexity of the algorithms for DOA estimation [1–5]. The performance analysis of most of these methods is carried out through numerical simulations. However, the practical significance of the DOA estimation problem demands real-time testing through actual hardware experiments for verification and validation of the methods. In this context, we have recently proposed a QR-TLS method for DOA estimation in [6] and presented its experimental verification in [7]. A smart antenna system implementation for DOA estimation has appeared in [8, 9] where the authors present an FPGA implementation of a DOA estimation algorithm with emulated sources. Another work in [10] implements the DOA estimator on a software defined radio (SDR). The authors discuss a phase calibration scheme to avoid estimation errors due to phase in-coherence between the RF receivers and tested the proposed DOA estimator in microwave anechoic chamber. In [11], the authors present a comparative study of the performance of DOA estimation of the MUSIC, Root-MUSIC, and ESPRIT algorithms [12–14] for the case of uncorrelated RF signals. For experimental testing, they use a receiving system composed of a linear array of antennas and a network of five-port demodulators operating at 2.4 GHz.

In this work, we present five methods of estimating DOA of multiple incident RF sources. The proposed methods rely on determining the signal and noise subspaces of either a unitary matrix Q upper

Received 23 January 2014, Accepted 1 April 2014, Scheduled 4 April 2014

* Corresponding author: Nizar Tayem (ntayem@pmu.edu.sa).

The author is with the Department of Electrical Engineering, College of Engineering Prince, Mohammad Bin Fahd University, Al-Khobar, Saudi Arabia.

triangle matrix R, or both Q and R matrices formed after the QR decomposition [15, 16] of a received signal data matrix.

Employing QR decomposition in the proposed methods has several advantages. Firstly, QR decomposition has lower computational complexity and it is less expensive than Singular Value Decomposition (SVD) which has been widely used in DOA methods such as MUSIC and ESPRIT. Secondly, QR factorization is an important tool in numerical linear algebra because it maintains accurate information about the data matrix rank and numerical null space and provides an efficient and robust solution for solving the least square problem which is widely used in array signal processing and spectral estimations [17–20]. Thirdly, implementation of QR decomposition with the Coordinate Rotation Digital Computer (CORDIC) algorithm requires only addition operations and shift registers [21], which improves the throughput and resource utilization. These advantages make proposed methods more suitable for high speed communication. The performance of the proposed methods is assessed through simulations as well as through hardware implementation of the proposed methods along with the two other well-known methods called MUSIC and ESPRIT on a NI PXI platform.

The NI PXI is a PC-based platform which features PCI electrical-bus, modular packaging, specialized synchronized buses and key software features. It is mainly used in industry for high-performance and low cost deployment of applications such as manufacturing, test, military and aerospace, machine monitoring, and automotive. Recently, it has also find its use in academics as a research tool [7]. The NI hardware used for the proposed DOA estimation methods consists of a chassis which includes a stand alone controller and modules with signal transmission/reception capabilities such as RF signal generator, RF down converter, digitizer, and RF amplifier, etc.. A uniform linear array (ULA) is constructed using four omni-directional antennas and it is interfaced with the NI-PXI platform. A phase calibration step is performed prior to the DOA estimation to remove any phase in-coherence between the RF receivers caused by the independent clocks of the receiver modules and the difference in receiver wire lengths. The proposed DOA estimation methods are tested in an open atmosphere. The experimental procedures are described in detail and the measurement results are shown which confirm the accuracy of the proposed DOA estimation methods.

The paper is organized as follows. Section 2 develops a system model for the DOA estimation problem. In Section 3, we present the details of the five proposed DOA estimation methods. The experimental setup and procedures are discussed in details in Section 4 followed by the experimental results in Section 5. We conclude the paper in Section 6.

2. SYTEM MODEL

A uniform linear array (ULA) consisting of four omni-directional antennas is shown in Figure 1. It is used in a real-time implementation of the proposed DOA estimation methods, MUSIC, and ESPRIT. The distance between the adjacent antennas is 16 cm which is equivalent of having the wavelength of 900 MHz. Single and multiple narrowband sources are considered for testing using real hardware and LabVIEW software.

To derive the mathematical model of the received signal, we consider L number of incident sources present in the far-field region of a ULA consisting of m elements. The sources are assumed to be lying

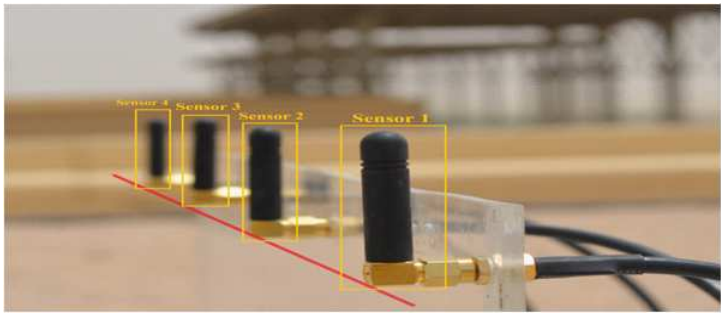

Figure 1. Uniform linear array consisting of four omni-directional antennas.

at the angles of $\theta_1, \theta_2, \ldots, \theta_L$. At any time instant t, the snapshot of the signal received at the ULA can be expressed as:

$$y_m(t) = \sum_{i=1}^{L} s_i(t)\ e^{-j(2\pi/\lambda)dm\cos\theta_i} + n_m(t) \tag{1}$$

where $s_i(t)$ is the signal from the i-th incident source, λ the wavelength, $(d = \lambda/2)$ the spacing distance of ULA, and $n_m(t)$ the noise at the m-th element.

The received vector can be modeled as

$$Y(t) = A(\theta)\, S(t) + N(t), \tag{2}$$

where $A(\theta)$ is the $(M \times L)$ array response matrix given as

$$A(\theta) = [\ \mathbf{a}(\theta_1) \quad \mathbf{a}(\theta_2) \quad \ldots \quad \mathbf{a}(\theta_L)\ ], \tag{3}$$

where $\mathbf{a}(\theta_i)$ for $i = 1, 2, \ldots, L$ is the corresponding array response vector.

$$a(\theta_L) = \left[\ 1 \quad \ldots \quad u_L^M\ \right]^T, \tag{4}$$

where

$$u_k = \exp\left(-j2\pi\ d\cos\left(\theta_k\right)/\lambda\right), \tag{5}$$

$S(t)$ is the vector of received signals given by

$$S(t) = [\ s_1(t) \quad s_2(t) \quad \ldots \quad s_L(t)\ ]^T, \tag{6}$$

and

$$N(t) = [\ n_1(t) \quad \ldots \quad n_M(t)\ ], \tag{7}$$

is the $(M \times 1)$ additive white Gaussian noise (AWGN) vector whose components have zero mean and a variance equal to σ^2. Here and in the following the superscripts T and * denote the transpose and conjugate operations, respectively.

3. PROPOSED DOA ESTIMATION METHODS

In the proposed methods, the information about the DOAs of incident sources can be extracted from Q matrix, R matrix, and the combination of Q and R matrices. Least square (LS) approach of finding the direction matrix is replaced with a total least square (TLS) method which is more appropriate under noisy measurements of practical scenarios. Detailed information about the proposed methods is given in the following subsections.

3.1. Method 1: Extract DOAs from the Data Matrix Q with Searching Technique

Estimation of the covariance matrix R_{YY} can be achieved through a collection of finite data samples as follows.

$$R_{YY} = E\left[Y(t)Y^H(t)\right] = ASA^H + \sigma^2 I \tag{8}$$

where the subscript H denotes conjugate transpose, $E[\ ]$ the expectation value, $S = E(S(t)S(t)^H)$ the covariance matrix of incident sources, I an identity matrix, and σ^2 the variance of additive white Gaussian noise.

The QR decomposition of the measured covariance matrix R_{YY} can be written as

$$R_{YY} = QR = [\ Q_s \quad Q_n\ ] \begin{bmatrix} R_L \\ O \end{bmatrix} \tag{9}$$

$Q_s = [q(1)\ q(2)\ \ldots\ q(L)]$ is the column vectors of signal space, $Q_n = [q(L+1)\ q(L+2)\ \ldots\ q(M)]$ is the column vectors of noise space, R_L an $(L \times M)$ matrix representing signal space, and O an $(M - L) \times M$ null matrix. Using the fact that Q is an orthonormal and unitary matrix, if we multiply both sides of Equation (9) by Q^H, we get:

$$\begin{bmatrix} Q_s^H R_{YY} \\ Q_n^H R_{YY} \end{bmatrix} = \begin{bmatrix} R_L \\ O \end{bmatrix} \tag{10}$$

Equation (10) can be written as:

$$Q_n^H A S A^H = O \tag{11}$$

Since A is a full rank and S a non-singular matrix for uncorrelated sources, it follows that

$$Q_n^H A = O \tag{12}$$

Equation (11) implies that the $M - L$ column vectors of Q_n are perpendicular to the columns vectors of A and span the same space.

$$span\,(\,q(L+1) \quad q(L+2) \quad \ldots \quad q(M)\,) = span(\,a(\theta_1) \quad a\,(\theta_2) \quad \ldots \quad a\,(\theta_L)) \tag{13}$$

Steering vectors corresponding to the direction of arrivals are orthogonal to the noise space. The DOAs can be found by searching for the minimum peaks of $\|Q_n^H A(\theta)\|$ by changing θ in the range of $(0, \pi)$. Equivalently, we can locate the peaks of the spatial spectrum which is defined as follows:

$$P\,(\theta) = \frac{1}{\|Q_n^H A(\theta)\|} = \frac{1}{A^H\,(\theta)\,Q_n^H Q_n A\,(\theta)} \tag{14}$$

The functional block diagram for implementing the proposed method 1 is summarized in Figure 2.

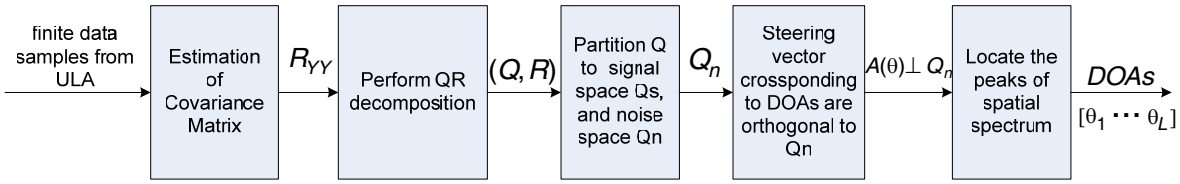

Figure 2. Block diagram of method 1 for DOA estimation.

3.2. Method 2: Extract DOAs from the Data Matrix *R* with Searching Technique

In this method, we employ the rank revealing QR factorization (RRQR) of the covariance matrix R_{YY}. The factorization of R_{YY} can be written as:

$$R_{YY} = QR = Q \begin{bmatrix} R_{11} & R_{12} \\ 0 & R_{22} \end{bmatrix}, \tag{15}$$

where R_{11} is $(L \times L)$, R_{12} is $(L \times (M - L))$, and R_{22} is $(M - L) \times (M - L)$. The QR factorization in (15) is called rank-revealing QR factorization. Since R_{22} is very small, the approximation of the data matrix R can be written as follows:

$$\hat{R} = [\ R_{11} \quad R_{12}\ ] \tag{16}$$

The data matrix in (16) represents the null space of R_{YY}. If a vector X belongs to the null space of $\hat{R}$, then the matrix $\hat{R}$ represents the set of all solutions to the following homogenous equation.

$$\hat{R}G = [\ R_{11} \quad R_{12}\ ] \begin{bmatrix} X_1 \\ X_2 \end{bmatrix} = 0 \tag{17}$$

where X_1 has L components, and X_2 has $L-M$ components. Since the data matrix R_{11} is a non-singular matrix for uncorrelated sources, the solution of (17) can be obtained as follows:

$$X_1 = \left(-R_{11}^{-1} R_{12}\right) X_2 \tag{18}$$

Using Equation (18), the vector X can be written as:

$$X = \begin{bmatrix} X_1 \\ X_2 \end{bmatrix} = \begin{bmatrix} -R_{11}^{-1} R_{12} \\ I_{L-M} \end{bmatrix} X_2 \tag{19}$$

The basis for the null space of the upper triangular matrix R which is also the null space of R_{YY} is, therefore, given by:

$$\psi = \begin{bmatrix} -R_{11}^{-1}R_{12} \\ I_{N-L+1} \end{bmatrix} \tag{20}$$

The columns of the null space of ψ are not orthonormal. We use orthogonal projection onto this subspace to satisfy orthonormality and to improve the performance by making the basis of null space of ψ orthonormal.

$$\psi_O = \psi \left(\psi^H \psi^{-1}\right) \ \psi^H \tag{21}$$

To estimate the DOAs, a search algorithm [12] similar to MUSIC is applied using the following function:

$$P(\theta) = \frac{1}{A^H(\theta)\,\psi_O A(\theta)} \tag{22}$$

where the peak positions indicate the DOAs of the incident sources.

Functional block diagram for implementing method 2 is explained in Figure 3.

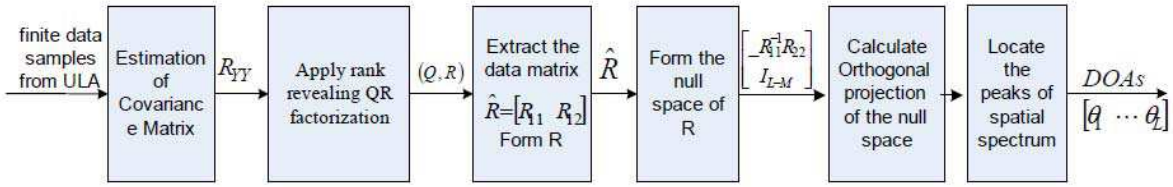

Figure 3. Block diagram of method 2 for DOA estimation.

3.3. Method 3: Extract DOAs from *R* Matrix Exploiting the Shift Invariant Property of the Array

In this method, RRQR factorization is employed to estimate the data matrix R. The following steps show the proposed method in details.

Step 1: Apply QR factorization on data matrix R_{YY}

$$R_{YY} = QR = Q \begin{bmatrix} R_{11} & R_{12} \\ 0 & R_{22} \end{bmatrix} \tag{23}$$

Step 2: Extract the first L rows of the data matrix R as follows:

$$Z_s = \begin{bmatrix} R_{11} \\ R_{12} \end{bmatrix} \tag{24}$$

The data matrix Z_s with dimension $(M \times L)$ will be used to estimate the DOAs.

Step 3: Partition Z_s datamatrix into two $((M-1) \times L)$ sub-matrices such that:

$$\begin{aligned} Z_{s1} &= Z_s(1 : M-1, :), \\ Z_{s2} &= Z_s(2 : M, :) \end{aligned} \tag{25}$$

Since range of $\Re[Z] = \Re[A]$, there must exist a unique matrix T, such that:

$$Z_s = \begin{bmatrix} Z_{s1} \\ Z_{s2} \end{bmatrix} = \begin{bmatrix} A_1 T \\ A_1 \phi T \end{bmatrix}, \tag{26}$$

where

$$A_1(\theta) = [\ \mathbf{a}_1(\theta_1) \quad \mathbf{a}_1(\theta_2) \quad \ldots \quad \mathbf{a}_1(\theta_L)\ ], \tag{27}$$

is the $((M-1) \times L)$ array response matrix, and where

$$a_1(\theta_L) = [\ 1 \quad \ldots \quad u_L^{M-1}\ ]^T \tag{28}$$

and ϕ is an $(L \times L)$ diagonal matrix containing information about the DOAs of incident sources.

$$\phi = \text{diag}\left[\begin{array}{ccc} e^{-\frac{j2\pi d\cos(\theta_1)}{\lambda}} & \ldots & e^{-\frac{j2\pi d\cos(\theta_L)}{\lambda}} \end{array}\right] \tag{29}$$

It can be easily seen that $\Re[Z_{s1}] = \Re[Z_{s2}] = \Re[A_1]$. Since Z_{s1} and Z_{s2} span the same signal space, it follows that they are related by a nonsingular transform Ω as follows:

$$Z_{s2} = Z_{s1}\Omega_1 \tag{30}$$

Since A is a full rank for uncorrelated sources, Equation (30) can be expressed as:

$$\Omega_1 = T^{-1}\phi\, T \tag{31}$$

The Eigenvalues of the matrix Ω_1 are the diagonal elements of ϕ. Finding the eigen-values of Ω_1 will lead to obtaining the DOAs for incident sources.

Equation (30) can be solved using least square approach (LS-ESPRIT) which minimizes the difference between Z_{s2} and $Z_{s1}\Omega_1$

$$\Omega = \arg\min_{(\Omega)} \|Z_{s2} - Z_{s1}\Omega\|_F^2 = \arg\min_{(\Omega)} tr\left\{[Z_{s2} - Z_{s1}\Omega]^H [Z_{s2} - Z_{s1}\Omega]\right\} \tag{32}$$

The least square solution of (32) can be found as:

$$\Omega = \left[Z_{s1}^H Z_{s1}\right]^{-1} Z_{s1} Z_{s2} \tag{33}$$

The solution in (33) is based on the assumption that errors only occur in Z_{s2}. Because both Z_{s2} and Z_{s1} contain errors, the more appropriate solution for (31) is a total least square (TLS) approach [16]. We can get the TLS solution of Ω in the following steps:

Step 4: Construct a new matrix using the sub-matrices signal space Z_{s1} and Z_{s2} as follows:

$$Z_{new} = \left[\begin{array}{cc} Z_{s1} & Z_{s2} \end{array}\right], \tag{34}$$

where the dimension of the data matrix Z_{new} is $((M-1) \times 2L)$.

Step 5: Apply second QR factorization on the matrix formed as:

$$QR\left[\left[\begin{array}{c} Z_1^H \\ Z_2^H \end{array}\right]\left[\begin{array}{cc} Z_1 & Z_2 \end{array}\right]\right] = QR\left[\begin{array}{cc} Z_1^H Z_1 & Z_1^H Z_2 \\ Z_2^H Z_1 & Z_2^H Z_2 \end{array}\right] = Q_2 R_2 \tag{35}$$

where Q_2 and R_2 are $(2L \times 2L)$ matrices.

Step 6: Partition R_2 into four $L \times L$ sub-matrices such that:

$$R_2 = \left[\begin{array}{cc} R_{211} & R_{212} \\ R_{221} & R_{222} \end{array}\right] \tag{36}$$

Step 7: Calculate the eigenvalues using the eigen decomposition of H matrix as follows:

$$H = -R_{212}R_{222}^{-1} \tag{37}$$

Step 8: Estimate the DOAs of multiple incident sources using the following expression:

$$\theta_L = \cos^{-1}\left(\frac{angle\left((\lambda_L)_H\right)}{2\pi d}\right) \tag{38}$$

The functional block diagram for implementing method 3 is explained in Figure 4.

3.4. Method 4: Extract DOAs from *Q* Data Matrix Exploiting the Shift Invariant Property of the Array

The output data matrix Q from the RRQR and shift invariant rotational property of the array will be used to estimate the DOAs of incident sources as follows:

Step 1: Apply QR decomposition on the data matrix R_{YY}

$$[Q, R] = qr\left[R_{YY}\right] = \left[\begin{array}{cc} Q_s & Q_n \end{array}\right] R, \tag{39}$$

where Q_s and Q_n are $(M \times L)$ and $(M \times (M-L))$ matrices, respectively.

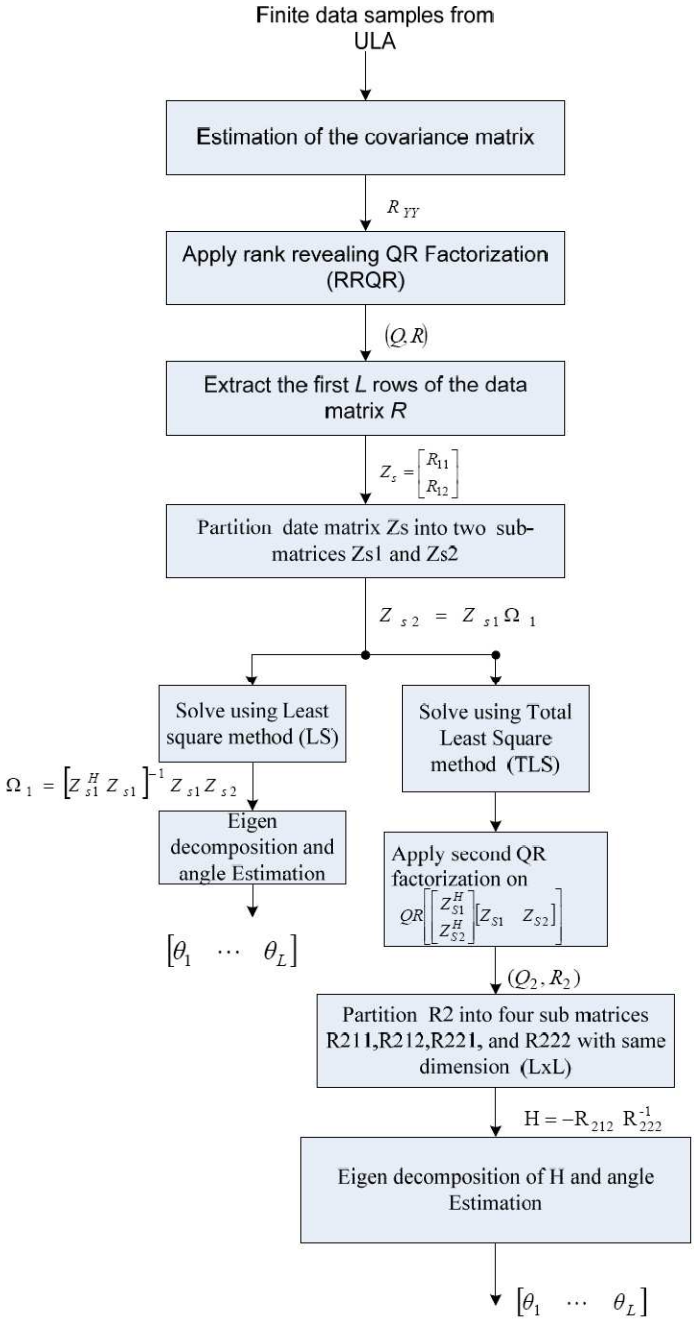

Figure 4. Block diagram of method 3 for DOA estimation.

The signal space Q_S can be obtained by selecting the first L columns of the Q matrix.

$$Q_s = [\ q(1) \quad q(2) \quad \ldots \quad q(L)\ ] \tag{40}$$

where $q(i)$ denotes the ith column of Q.

Step 2: Partition the Q_s matrix into two sub matrices Q_{s1} and Q_{s2} as follows:

$$Qs = [\ Q_{s1} \quad Q_{s2}\ ] \tag{41}$$

where $Q_{s1} = Q_s(1 : M-1, L)$ and $Q_{s2} = Q_s(2 : M, L)$.

Since Q_{s1} and Q_{s2}, span the same signal space, they are related by a nonsingular transform Ω_2 as follows:

$$Q_{s2} = Q_{s1}\Omega_2 \tag{42}$$

The LS (least square) solution of (42) can be found as:

$$\Omega_2 = \left[Q_{s1}^H Q_{s1}\right]^{-1} Q_{s1} Q_{s2} \tag{43}$$

Additional steps are required to find the TLS solution of (42) as follows:

Step 3: Apply second QR decomposition on the matrix formed as:

$$QR\left[\begin{bmatrix} Q_{s1}^H \\ Qs2 \end{bmatrix}\begin{bmatrix} Q_{s1} & Q_{s2} \end{bmatrix}\right] = QR\begin{bmatrix} Q_{s1}^H Q_{s1} & Q_{s1}^H Q_{s2} \\ Q_{s2}^H Q_{s1} & Q_{s2}^H Q_{s2} \end{bmatrix} = Q_T R_T \tag{44}$$

Q_T and R_T are $(2L \times 2L)$ matrices.

Step 4: Partition Q_T into four sub-matrices with same size $(L \times L)$

$$Q_T = \begin{bmatrix} Q_{11} & Q_{12} \\ Q_{21} & Q_{22} \end{bmatrix} \tag{45}$$

Step 5: Compute the eigenvalues (λ's) of the matrix W given as:

$$W = -Q_{12} Q_{22}^{-1} \tag{46}$$

Step 6: Estimate the DOAs of multiple incident sources using the following expression:

$$\hat{\theta}_k = \cos^{-1}\left(\frac{angle\left((\lambda_L)_W\right)}{2\pi d}\right) \tag{47}$$

where $\hat{\theta}_k$ is the estimated DOA of the kth source for $k = 1, 2, \ldots, K$. The functional block diagram for implementing method 4 is explained in Figure 5.

3.5. Method 5: Extract the DOAs from the Combination of *R* and *Q* Matrices Exploiting the Shift Invariant Property of the Array

DOAs can be obtained in method 3 and method 4 by using R and Q matrices respectively. While in this method the information about DOAs can be found from the combination of R and Q matrices. The following steps explain the proposed method.

Step 1: Perform QR decomposition on the data matrix R_{YY} as in Equation (15).

$$[q_1, r_1] = QR\left[R_{YY}\right] = Q\begin{bmatrix} R_{11} & R_{12} \\ 0 & R_{22} \end{bmatrix} \tag{48}$$

Step 2: Define a new data matrix F with dimension $(M \times L)$ using the result of Equation (48) as follows:

$$F = \begin{bmatrix} R_{11} & R_{12} \end{bmatrix} \tag{49}$$

The data matrix in (49) represents a new filtered data version which mainly corresponds to the signal space.

Step 3: Calculate the second QR decomposition of F^H

$$[q_2, r_2] = QR\left[F^H\right] \tag{50}$$

where q_2 and r_2 are $(M \times M)$ and $(L \times L)$ matrices of the signal space, respectively.

Step 4: Express the second QR decomposition in its signal space part as:

$$F_S = \left[q_2\left(:, 1:L\right)\right]\left[r_2\left(1:L, 1:L\right)\right],$$

where F_S is $(M \times L)$.

Step 5: Partition the F_S matrix into two sub matrices F_{s1} and F_{s2} as follows:

$$Fs = \begin{bmatrix} F_{s1} & F_{s2} \end{bmatrix} \tag{51}$$

where $F_{s1} = F_s(1 : M-1, L)$ and $F_{s2} = F_s(2 : M, L)$.

Since F_{s1} and F_{s2}, span the same signal space, they are related by a nonsingular transform Ω_2 as follows:

$$F_{s2} = F_{s1}\Omega_3 \tag{52}$$

To estimate the DOAs of incident sources, TLS and LS methods can be applied as in methods 4 and 5.

The functional block diagram for implementing method 5 is explained in Figure 6.

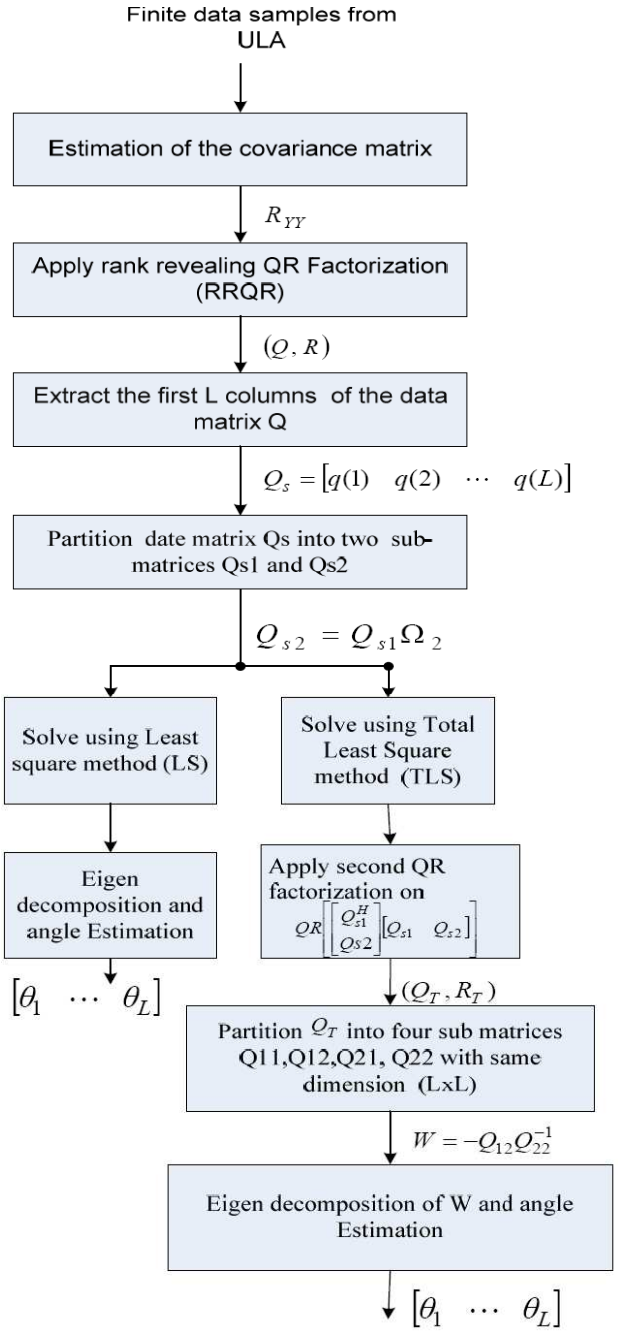

Figure 5. Block diagram of method 4 for DOA estimation.

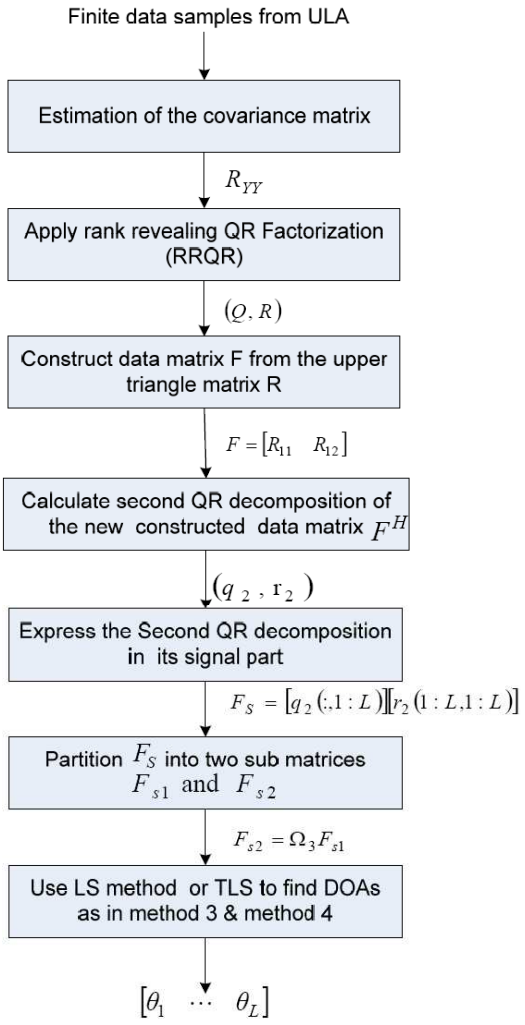

Figure 6. Block diagram of method 5 for DOA estimation.

4. EXPERIMENTAL SETUP

The proposed methods are verified experimentally by building a test setup on a flat roof of a university building to emulate open atmospheric conditions with minimal reflecting surfaces. The hardware implementation of the proposed methods on the NI PXI platform is performed in two steps. In the first step, the physical connections are made between the NI PXI modules and the transmitter/receiver antennas. In the next step, a phase calibration process is performed to co-phase the receiver end antennas. The details of these steps are presented in the following sub-sections.

4.1. Setting up an RF Transmitter

The block diagram of the NI PXI transmitter end is shown in Figure 7 [7]. A digital signal is generated in the first stage using LabView built-in functions which includes source coding, channel coding, and modulation. The digital signal thus generated, is passed through arbitrary waveform generator (AWG) which converts it into an analog signal. The up-converter module transforms the analog signal from an intermediate frequency (IF) to a radio frequency (RF) signal which is later amplified prior to the signal transmission via antenna.

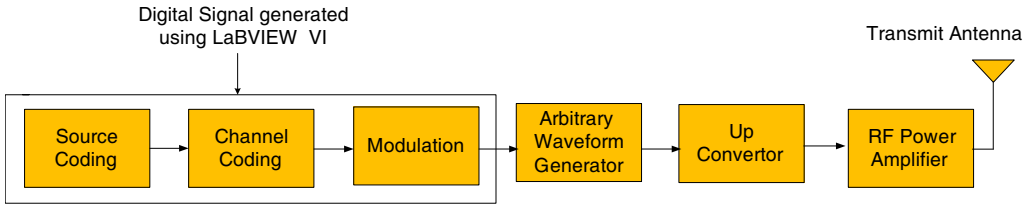

Figure 7. Block diagram of the NI-PXI transmitter unit.

The front panel of the LabView code developed for the transmitter unit is shown in Figure 8. It can be seen that the modulation scheme selected for the transmitted signal is QPSK. The modulated signal is up-converted to a center frequency of 900 MHz and transmitted with a power level of 10 dBm. The figure also shows the constellation diagram of the QPSK modulated signal.

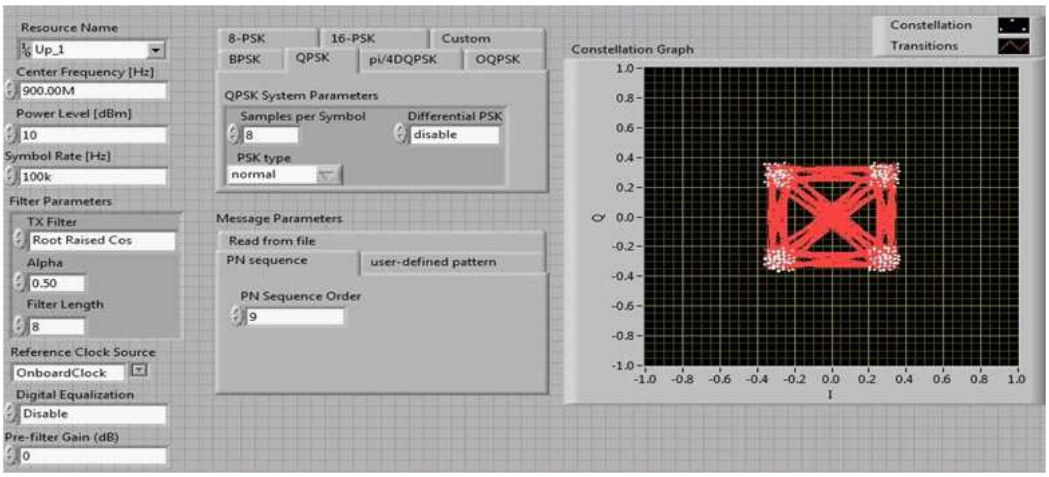

Figure 8. Front panel of the transmitter end LabVIEW code.

4.2. Setting up an RF Reciver

The receiver end consists of a ULA of four omnidirectional wire antennas, RF down-converter (PXIe-5601) and high speed digitizer (PXIe-5622) modules. The antennas are connected to RF down-converter module (NI PXIe-5601). Each of the four RF down-converter modules has an input for a local oscillator (LO) which is connected to the same clock signal generated by an RF signal generator module (NI PXIe-5652). The block diagram of the NI-PXI configured as an RF receiver is shown in Figure 9.

4.3. Phase Calibration at the Receiver End

The DOA estimation methods extract the directional information of the source signal from the phase shifted copies of the source signal received at the antennas of the ULA. Thus, in order to avoid estimation errors, it is extremely important to co-phase the receiving antennas. Detailed information about the phase calibration mechanism is thoroughly explained in [7].

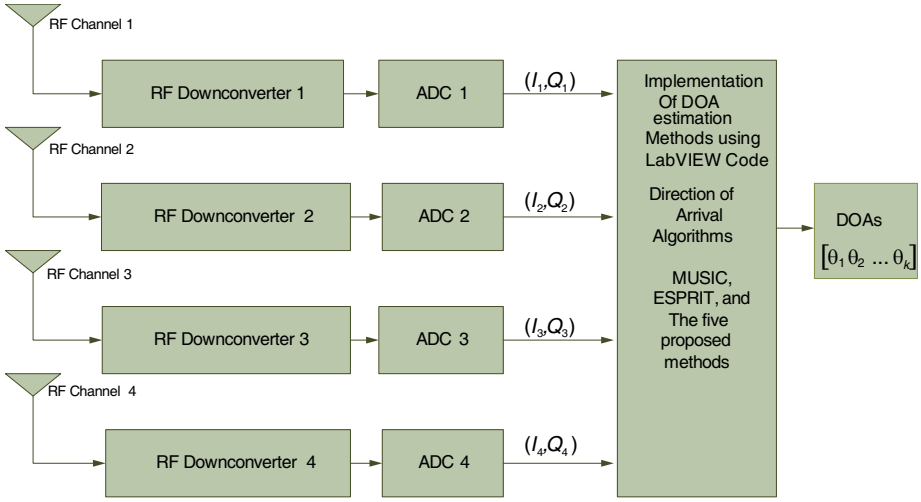

Figure 9. Block diagram of the NI-PXI receiver unit.

5. SIMULATION AND EXPERIMENTAL RESULTS

The performance of the proposed DOA estimation methods is verified through both numerical simulations and by conducting experiments in real-time. Two separate cases are considered with a single source and two sources placed at arbitrarily selected angles from the array reference. The numerical simulation for three sources is also considered.

5.1. Simulation Results

5.1.1. Single RF Incident Source

The first case assumes a single RF source placed in the far-field region of a ULA at an angle of 100° from the array reference composed of four antennas and the SNR set to 5 dB. For ease of plotting and visualization, the simulations results of the proposed methods 1, 2, and MUSIC are grouped together while the other group is formed for the results of the proposed methods 3, 4, 5, and ESPRIT method. Figure 10 shows the spectrum of the angle estimates obtained for the group 1 methods. The DOA

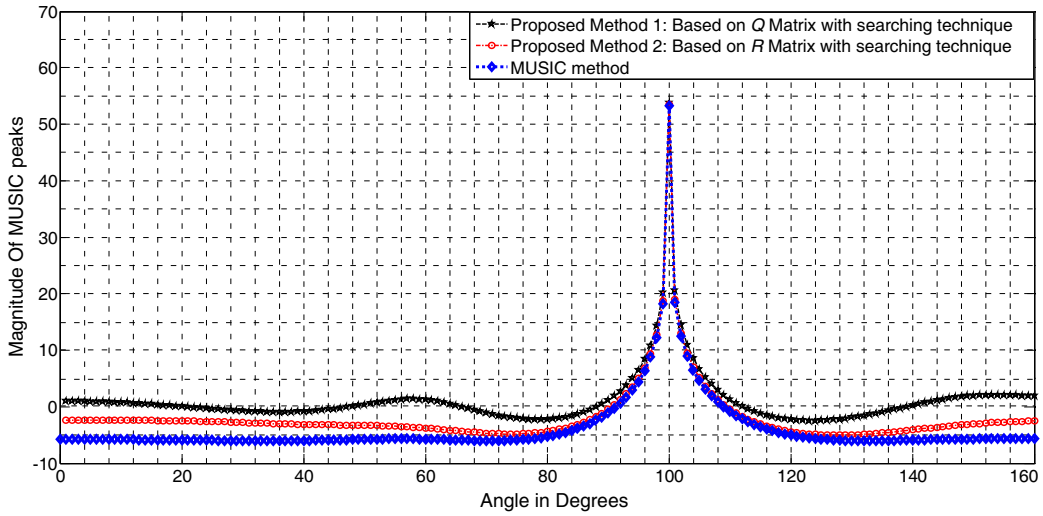

Figure 10. Simulated DOA estimates of the proposed methods 1, 2 and MUSIC for single source lying at 100° from the array reference.

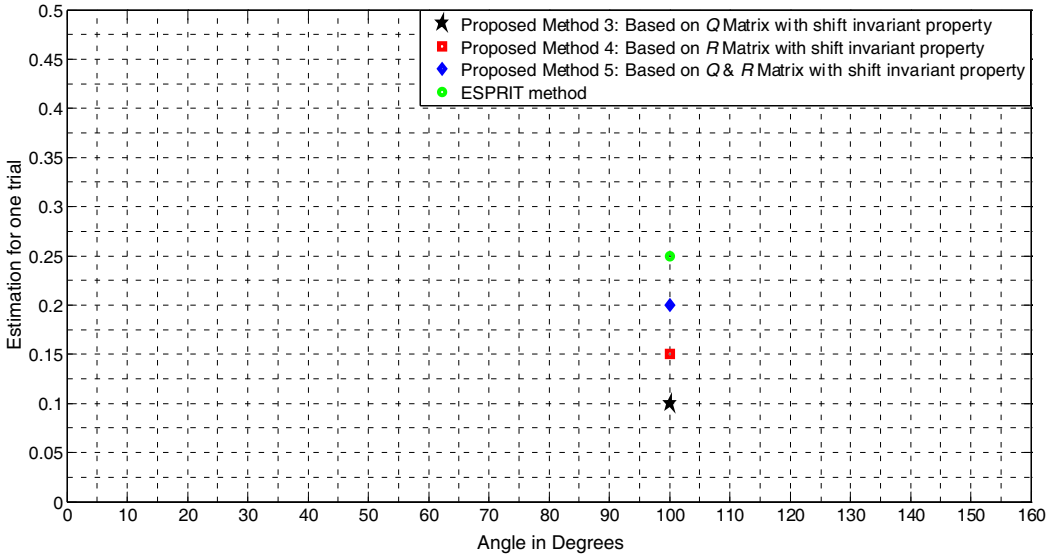

Figure 11. Simulated DOA estimates of the proposed methods 3, 4, 5 and ESPRIT for single source lying at 100° from the array reference.

estimate corresponds to the peak of the spectrum which for all the methods can be seen close to the actual angle. The DOA estimates obtained with the group 2 methods are shown in Figure 11. It can be seen that accurate estimates are obtained with both the proposed methods and the ESPRIT method.

5.1.2. Two RF Incident Sources

The case of two sources is also considered in simulations where the sources are assumed to be lying in the far-field region of a ULA at angles of 37° and 115° from the array reference. The estimated angles for the group 1 methods are shown in Figure 12. The figure shows the spectrum with two peaks, where the peaks can be seen to provide precise angle estimates. Similar is the case with the group 2 methods as shown in Figure 13 which shows close match with the actual angles.

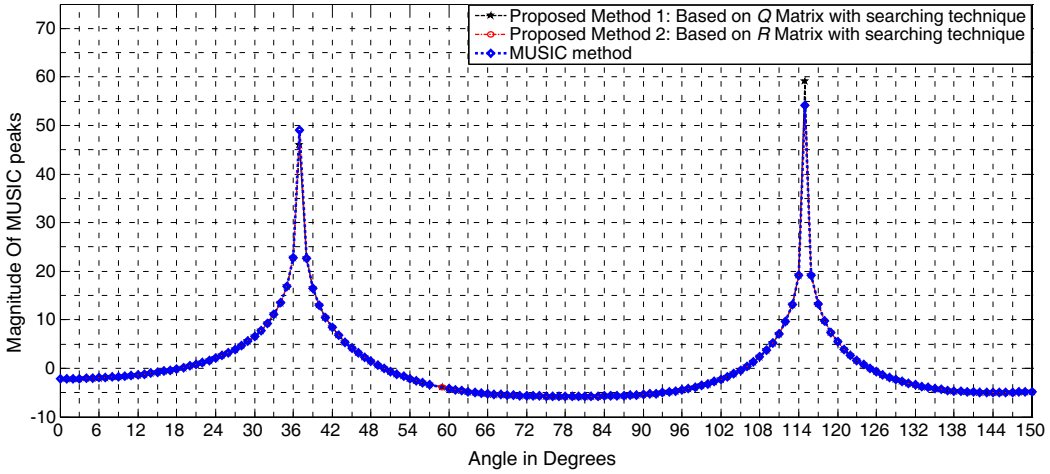

Figure 12. Simulated DOA estimates of the proposed methods 1, 2, and MUSIC for two sources lying at 37° and 115° from the array reference.

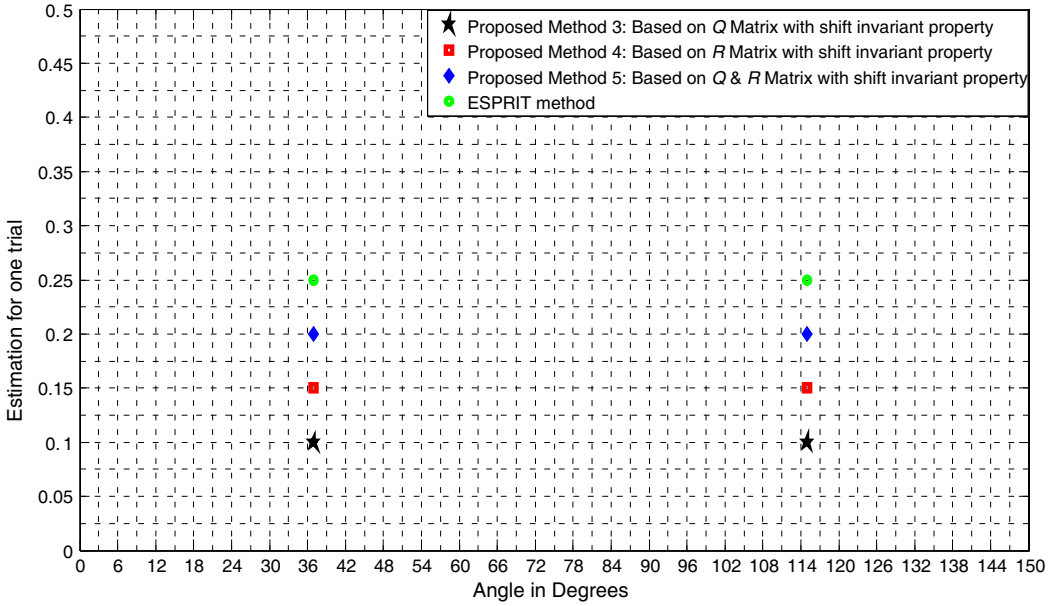

Figure 13. Simulated DOA estimates of the proposed methods 3, 4, 5 and ESPRIT for two sources lying at 37° and 115° from the array reference.

5.1.3. Multiple RF Incident Sources

The case of three sources is also considered in simulations where the sources are assumed to be lying in the far-field region of a ULA at angles of 45°, 60° and 75° from the array reference composed of six antennas. We observe in Figure 14 that proposed methods 1 and 2 provide precise estimation of the three peaks appearing at 45°, 60° and 75°. Also, Figure 15 shows that proposed methods 3, 4, and 5 can estimate the DOAs of multiple sources with high accuracy.

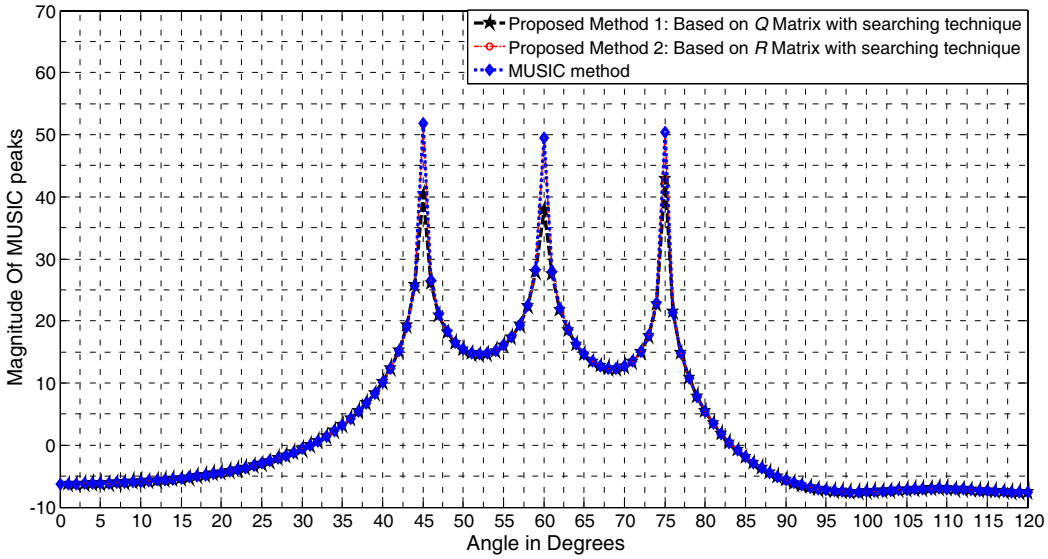

Figure 14. Simulated DOA estimates of the proposed methods 1, 2, and MUSIC for three sources lying at 45°, 60° and 75° from the array reference.

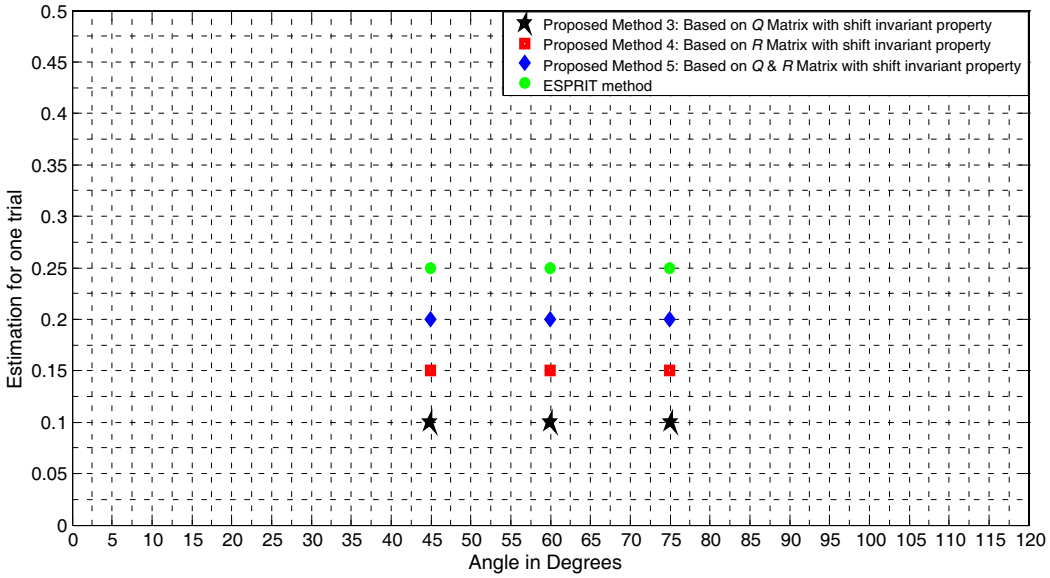

Figure 15. Simulated DOA estimates of the proposed methods 3, 4, 5, and ESPRIT for three sources lying at 45°, 60° and 75° from the array reference.

5.1.4. Comparison of Computational Time of Proposed Methods with MUSIC and ESPRIT Methods

Table 1 lists the computational time of various numbers of snapshots (500, 1000 and 1500) for MUSIC, ESPRIT, and the proposed methods considering 100 trials and three incident sources. In group 1 with searching techniques, we observe that proposed methods 1 and 2 have less computational time than

Table 1. Comparison of computional time for MUSIC method, ESPRIT method, and proposed methods using different numbers of snapshots and 100 trials.

Group	**DOA Estimation methods**	Computational time in seconds for 500 snapshots	Computational time in seconds for 1000 snapshots	Computational time in seconds for 1500 snapshots
Group 1	**MUSIC Method**	1.6758	2.6351	3.9453
	Proposed Method 1 Q Matrix with searching technique	1.3799	2.3463	3.5395
	Proposed Method 2 R Matrix with searching technique	1.2530	2.3605	3.4189
Group 2	**ESPRIT Method**	0.8055	1.3434	1.7564
	Proposed Method 3 Q Matrix with shift invariant property	0.6599	1.0965	1.3680
	Proposed Method 4 R Matrix with shift invariant property	0.5291	1.0295	1.3342
	Proposed Method 5 Q & R Matrix with shift invariant property	0.6587	1.0814	1.3554

MUSIC method. Also, the proposed methods 3, 4, and 5 in group 2 with shift invariant property requires less computational time than ESPRIT method. This verifies that proposed methods are more appropriate for high speed communication. Another observation from Table 1 is that the estimation of DOAs using searching techniques as in proposed methods 1 and 2 requires more than double the time needed using methods 3, 4, and 5 with shift invariant property. The principal reason why proposed methods 3, 4, and 5 have less running time than proposed methods 1 and 2 is that no searching is required to estimate the DOAs in methods 3, 4, and 5.

5.2. Experimental Results

5.2.1. Single RF Incident Source

The experimental configuration for the first case is shown in Figure 16, where a single RF source is placed in the far-field region of a ULA at an angle of 100° from the array reference. The source is placed

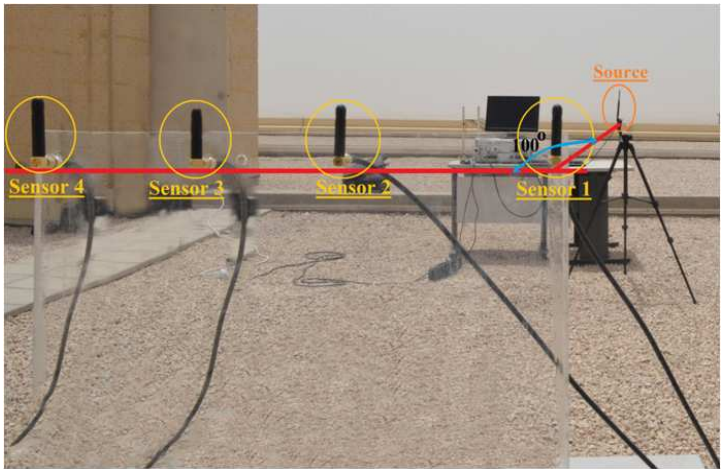

Figure 16. Experimental configuration for a single RF source placed at 100° from the array reference.

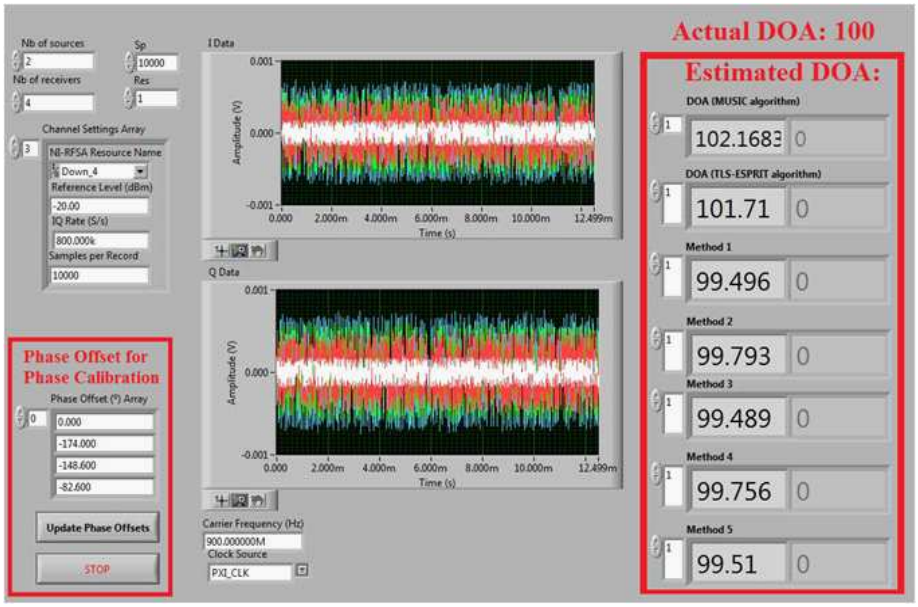

Figure 17. Experimental results for a single RF source placed at 100° from the array reference.

at the desired angle (which in the first case is 100°) by manually measuring the angle with a protractor and a string extended from the source antenna to the first antenna of the ULA which is considered as an array reference.

The experimental results of the existing MUSIC and ESPRIT algorithms along with the five proposed methods for the first test case with a single RF source are shown in Figure 17. The estimated angle of arrivals obtained with the MUSIC and ESPRIT are 102.16° and 101.71°, respectively. The figure also shows the direction of arrival estimates for the five proposed method which are 99.49°, 99.79°, 99.48°, 99.75°, and 99.51°, respectively. From the results, we observe more accurate angle estimates with the proposed methods. The figure also shows the value of phase offsets which are necessary for the phase calibration between the multiple antennas of the ULA at the receiver end.

The received signal strengths for the first case of single RF source are shown in Figure 18. An average signal power of around 40 dBm is received which is an acceptable value for the received signal strength.

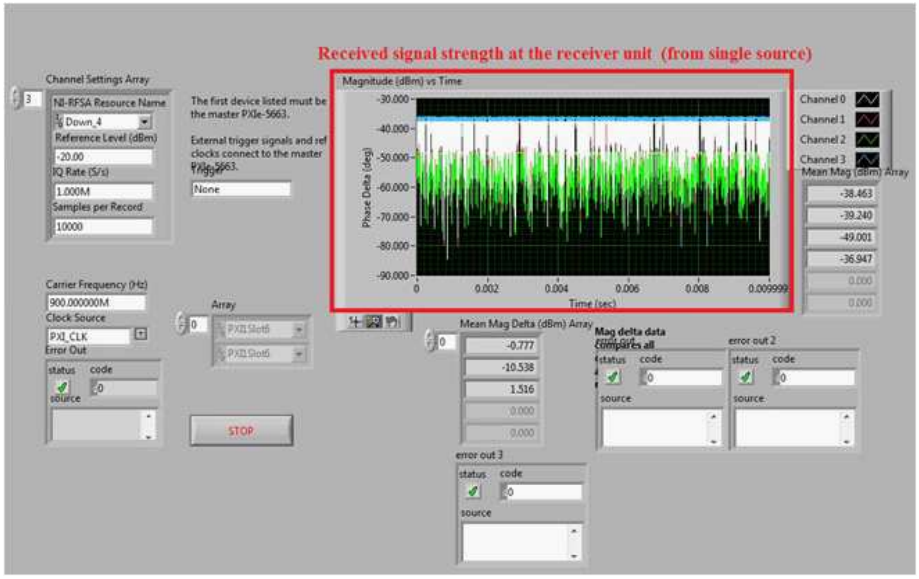

Figure 18. Received signal strength for a single RF source placed at 100° from the array reference.

Figure 19. Experimental configuration of two RF sources placed at 37° and 115° from the array reference.

5.2.2. Multiple RF Incident Sources

The performance of the proposed methods for DOA estimation of multiple incident sources is also evaluated experimentally. Figure 19 shows the experimental setup in which two RF sources are placed in the far-field region of a ULA. The sources are placed at manually measured angles of 37° and 115°, respectively from the array reference where the first antenna of the ULA is considered as an array reference. The lines drawn from the reference antenna to the sources represent the two angles of arrival.

The two DOA estimates obtained with the existing MUSIC and ESPRIT methods are (36.51°, 115.15°) and (36.26°, 114.25°), respectively as shown in Figure 20. The figure also shows the estimated angles of the proposed methods which are (34.87°, 114.48), (37.59°, 114.95°), (36.31°, 115°), (37.65°, 114.93°), and (36.30°, 113.64°), respectively. Thus, the DOA estimates obtained for the multiple incident source signals with the proposed methods are consistent with the actual measured angles. The signal strengths of the received signals for the case of two incident RF sources are also shown in Figure 21. The figure shows an average signal power of 43 dBm.

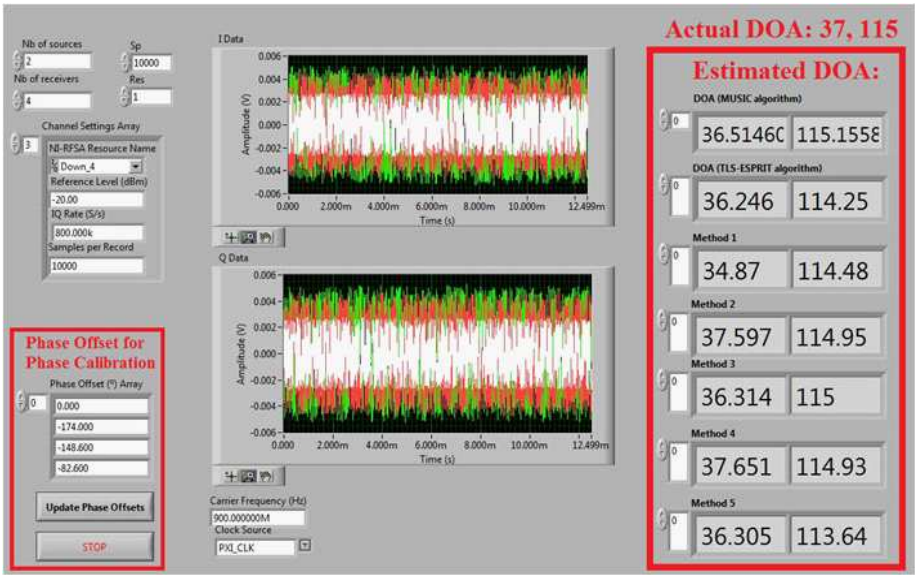

Figure 20. Experimental results for the two RF sources placed at 37° and 115° from the array reference.

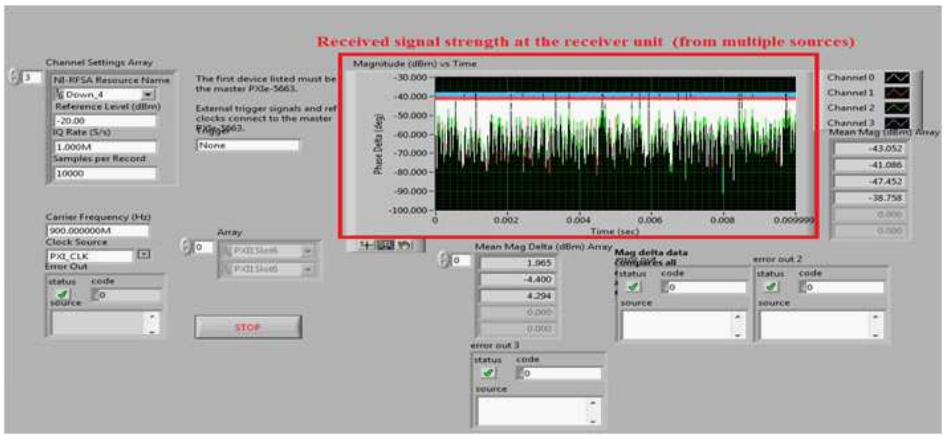

Figure 21. Received signal strength for the two RF sources placed at 37° and 115° from the array reference.

6. CONCLUSIONS

This paper presents five new methods of finding direction of arrival of multiple incident RF sources. The proposed methods extract angle information from the signal and noise subspaces obtained from either Q matrix, R matrix, or both Q and R matrices of the QR decomposed received data matrix. The performance of the proposed methods is verified through numerical simulations as well as through actual hardware experiments. The experimental procedures of hardware implementation of the proposed DOA estimation methods are described in detail. The results, shown for a single and two RF sources lying at arbitrary angles from the array reference, confirm successful real time implementation of the proposed DOA estimation methods. The performance of the proposed method is also verified for the case of multiple sources through numerical simulations.

REFERENCES

1. Zhang, Y., Z. Ye, X. Xu, and J. Cui, "Estimation of two-dimensional direction-of-arrival for uncorrelated and coherent signals with low complexity," *IET Radar, Sonar & Navigation*, Vol. 4, No. 4, 507, 2010.
2. Paulraj, A., R. Roy, and T. Kailath, "Estimation of signal parameters via rotational invariance techniques — ESPRIT," *Nineteeth Asilomar Conference on Circuits, Systems and Computers*, 83–89, 1985.
3. Yang, P., F. Yang, and Z.-P. Nie, "DOA estimation with sub-array divided technique and interporlated ESPRIT algorithm on a cylindrical conformal array antenna," *Progress In Electromagnetics Research*, Vol. 103, 201–216, 2010.
4. Kim, Y.-S. and Y.-S. Kim, "Improved resolution capability via virtual expansion of array," *Electronics Letters*, Vol. 35, No. 19, 1596, 1999.
5. Park, G.-M. and S.-Y. Hong, "Resolution enhancement of coherence sources impinge on a uniform circular array with array expansion," *Journal of Electromagnetic Waves and Applications*, Vol. 21, No. 15, 2205–2214, Jan. 2007.
6. Tayem, N., M. Omer, H. Gami, and J. Nayfeh, "QR-TLS ESPRIT for source localization and frequency estimations," *Asilomar Conference on Signals and Systems*, 2013.
7. Tayem, N., M. Omer, M. El-Lakkis, S. A. Raza, and J. F. Nayfeh, "Hardware implementation of a proposed Qr-Tls DOA estimation method and Music, ESPRIT Algorithms on Ni-Pxi platform," *Progress In Electromagnetics Research C*, Vol. 45, 203–221, 2013.
8. Ichige, K. and H. Arai, "Implementation of FPGA based fast DOA estimator using unitary MUSIC algorithm [cellular wireless base station applications]," *2003 IEEE 58th Vehicular Technology Conference. VTC 2003-Fall (IEEE Cat. No.03CH37484)*, Vol. 1, 213–217, 2003.
9. Ichige, K. and H. Arai, "Real-time smart antenna system incorporating FPGA-based fast DOA estimator," *IEEE 60th Vehicular Technology Conference, VTC2004-Fall*, Vol. 1, 160–164, 2004.
10. Wang, H. and M. Glesner, "Hardware implementation of smart antenna systems," *Advances in Radio Science*, No. 1, 185–188, 2006.
11. Osman, L., I. Sfar, and A. Gharsallah, "Comparative study of high-resolution direction-of-arrival estimation algorithms for array antenna system," Vol. 2, No. 1, 72–77, 2012.
12. Schmidt, R. O., "Multiple emitter location and signal parameter estimation," *IEEE Transactions on Antennas and Propagation*, Vol. 34, No. 3, 276–280, Mar. 1986.
13. Barabell, A. J., "Improving the resolution performance of eigenstructure based direction finding algorithms," *Proceedings of the ICASSP-83*, 336–339, 1983.
14. Roy, R. and T. Kailath, "ESPRIT estimation of signal parameters via rotational invariance techniques," *IEEE Transactions on Acoustics, Speech, and Signal Processing*, Vol. 29, No. 4, 984–995, Jul. 1989.
15. Horn, R. A. and C. Johnson, *Matrix Analysis*, Cambridge University Press, Cambridge, MA, 1985.
16. Golub, G. and C. F. van Loan, *Matrix Computations*, 3rd edition, 2715 North Charles Street, The John Hopkins University Press, Baltimore Maryland, 1996.

17. Verdú, S., *Multiuser Detection*, Cambridge University Press, Cambridge, MA, 1998.
18. Scharf, L., *Statistical Signal Processing: Detection, Estimation and Time Series Analysis*, Addison-Wesley Publishing Company, Inc, Reading, MA, 1991.
19. Poor, V., *An Introduction to Signal Detection and Estimation*, 2nd edition, Springer-Verlag, New York, 1989.
20. Björck, A., *Numerical Methods for Least Squares Problems*, SIAM, Philadelphia, 1996.
21. Lounici, M., X. Luanand, and W. Saadi, "Implementation of QR-decomposition based on CORDIC for unitary MUSIC algorithm," *Proc. SPIE 8878, Fifth International Conference on Digital Image Processing (ICDIP 2013)*, 88784L, 2013.